Global Dormancy of Metastases due to Systemic Inhibition of Angiogenesis

Sébastien Benzekry, Alberto Gandolfi, Philip Hahnfeldt

▶ **To cite this version:**

Sébastien Benzekry, Alberto Gandolfi, Philip Hahnfeldt. Global Dormancy of Metastases due to Systemic Inhibition of Angiogenesis. 2013. hal-00868592v2

HAL Id: hal-00868592

https://inria.hal.science/hal-00868592v2

Preprint submitted on 2 Oct 2013 (v2), last revised 27 Dec 2013 (v3)

HAL is a multi-disciplinary open access archive for the deposit and dissemination of scientific research documents, whether they are published or not. The documents may come from teaching and research institutions in France or abroad, or from public or private research centers.

L'archive ouverte pluridisciplinaire **HAL**, est destinée au dépôt et à la diffusion de documents scientifiques de niveau recherche, publiés ou non, émanant des établissements d'enseignement et de recherche français ou étrangers, des laboratoires publics ou privés.

Global Dormancy of Metastases due to Systemic Inhibition of Angiogenesis

Sébastien Benzekry[a,b], Alberto Gandolfi[c], Philip Hahnfeldt[a]

[a]*Center of Cancer Systems Biology, GRI, Tufts University School of Medicine, Boston, 02142, USA*
[b]*Inria team MC2, Institut de Mathématiques de Bordeaux, Bordeaux, France*
[c]*Istituto di Analisi dei Sistemi ed Informatica « Antonio Ruberti », Roma, Italy*

Corresponding author: Philip Hahnfeldt, philip.hahnfeldt@tufts.edu

Abstract

In autopsy studies of adults dying of non-cancer causes, virtually all were found to possess occult, but histologically confirmed, cancerous lesions. This suggests that, for most individuals, cancer will become dormant and not progress, while only in some will it become symptomatic disease. Meanwhile, it was recently shown in animal models that a tumor can produce both stimulators and inhibitors of its own blood supply. To explain the autopsy findings in light of the research data, we propose a mathematical model of cancer development at the organism scale describing a growing population of metastases, which, together with the primary tumor, exerts a progressively greater net systemic angiogenesis-inhibitory influence that collectively can suppress the growth of all lesions. *In silico* study of the dynamics of the system suggests that mutual inhibitory interactions within a population of tumors could yield to global dormancy of metastases. This last phenomenon is viewed as an organism-level homeostatic steady state of the total metastatic burden.

Author summary

Cancer does not always develop to become a clinically manifest disease. Most of the population actually carries small occult tumors that remain asymptomatic and undetectable. Here, we propose a theoretical study of this phenomenon by defining and simulating a novel mathematical model able to describe the development of a population of tumors at the organism scale. After demonstrating the model can explain experimental data on metastatic development, we go on to test the hypothesis of global dormancy resulting from inhibitory signaling interactions among the tumors. These interactions are targeted against the tumor's vascular support development (angiogenesis), known to be essential for tumor growth, by means of inhibitory molecules released in the circulation. By quantifying their consequences on the establishment of metastases and maintenance of the dormant state, our model shows for the first time how a previously unrecognized phenomenon – systemic inhibition of angiogenesis (SIA) – regulates tumor development. We show SIA alone is not sufficient for global dormancy but can suppress the growth of the total metastatic burden, even to the point of producing an equilibrium state with low and stable total cancerous mass.

Introduction

Almost all of us carry small tumor lesions that for many will not progress to symptomatic disease. Indeed, as evidenced in autopsy studies for adults without pre-established cancer such as [1,2], occult lesions are present in most healthy adults. Nielsen et al. [3] found that, out of 110 women cases, among which only one had been previously treated for breast cancer, 22% had at least one malignant lesion. Moreover, 45% of these had multicentric lesions. Similar results have been reported for prostate cancer in men [4]. For thyroid cancer, autopsy results [2] showed a prevalence rate of 99.9% for occult carcinomas, but incidence of thyroid cancer is only 0.1% of the population [5].

To explain these results, it is necessary to understand the tumor dormancy phenomenon. Tumor dormancy [6,7] is characterized by stable or very slow tumor growth. It can happen at the cellular level as a malignant cell remaining quiescent for a long period before awakening, but here we will focus on the mm-scale lesions that have surfaced in the several remarkable autopsy studies discussed, i.e., tissue-level tumor dormancy. Although the size of a dormant tumor remains almost constant, it is not due to a cessation in cell proliferation, but rather to increased apoptosis that leads to a near zero net growth rate [6–8]. Underlying molecular mechanisms tumor dormancy have been shown to relate to the balance between stimulation and inhibition of angiogenesis [7,9,10]. Clinically, tumor dormancy has been observed in breast cancer [3,11–13], melanoma [14] and prostate cancer [4], among many others [6]. Dormancy is particularly relevant to the situation where secondary tumors (metastases) remaining small and undetectable for extended periods.

Various explanations have been proposed for induction and maintenance of metastatic dormancy, among these being inhibition of the growth of the secondary tumors by a primary neoplasm, called concomitant resistance [15,16]. Although a distant impairment of metastatic growth by a primary tumor had already been observed over a hundred years ago [17], this phenomenon remains poorly understood, despite various preclinical [18–22] and clinical [11,23–25] studies.

Proposed theories to explain inhibition of secondary tumors by the primary are well summarized by Chiarella et al. [16]: 1) monopolization of certain resources by the primary tumor that deprives secondary tumors of materials needed for growth, 2) primary tumor-induced enhancement of immune suppression of small secondary tumors (concomitant immunity), 3) anti-proliferative molecules released by the primary tumors and 4) release of angiogenesis inhibitors by the primary tumor into the blood circulation resulting in inhibition of vascular development at secondary sites.

Because of evidence that concomitant resistance happens in immune-deficient mice [21] and considering the large and unequivocal body of support for the role angiogenesis inhibition plays in the maintenance of tumor dormancy [8,26–30] and the “angiogenic switch” [31] in escape from dormancy, we will focus on the

last theory. Angiogenesis, the process of creating new blood vessels and developing a supporting vascular network, was shown by Folkman [32] to be critical for tumor growth. Without development of new blood vessels, a malignant neoplasm cannot grow further than about 2 to 3mm in diameter, due to nutrient supply limitations [32]. This process is regulated by the release from cancer cells of growth factors such as vascular endothelial growth factor (VEGF) or basic fibroblast growth factor (bFGF) provoking proliferation, migration and maturation of surrounding endothelial cells. In 1994, O'Reilly et al. [26] were the first to discover an endogenous molecule having an inhibitory effect on angiogenesis, named angiostatin, followed soon by the discovery of endostatin [27] and thrombospondin-1 [29]. Overlaying the ability of tumors to stimulate vasculature, their ability to also inhibit it allows for the possibility that tumors may indirectly control their own growth [10,33], perhaps as a vestige of normal organ growth control. Further, inherent to this self-control notion, the inhibitors may be longer-lived and thus more persistent in the circulation, which could have the collateral effect of suppressing angiogenesis and growth at distant metastatic sites as the tumor mass gets large. Indeed, the half-life of stimulators has been reported to be on the order of minutes for VEGF [34], while that for inhibitors is on the order of hours [26,29].

Here we present a mathematical model for the description of such a phenomenon. Heretofore, while substantial efforts have been undertaken to take into account numerous complex mechanisms of cancer biology (see [35] for a review) very few mathematical models have been developed to describe their metastatic development, despite metastasis being the main cause of death from cancer [36]. Indeed, the cure rate of cancer before appearance of metastases is about 90% for all cancers combined, but falls to 15% when distant metastases are present at diagnosis [16]. As far as we know, modeling efforts in this direction can only be found in the work of Liotta and coworkers [37] and more recently in a few stochastic models [38–41] describing the progression through the different events of the metastatic process (cell detachment, intravasation, survival in the blood, extravasation, settling in a new environment). More than a decade ago, Iwata and coworkers [42] proposed a quantitative model for the development of metastatic colonies, which was of great potential interest as it is was designed to describe the size distribution of the metastases, allowing thus to distinguish between micro-metastases and larger lesions. However, this model does not take angiogenesis into account. Based on this work (which was shown to accurately describe data on regional metastases of a hepatocellular carcinoma in a patient) as well as on the model of Hahnfeldt et al. [10] for tumor development under angiogenic control, a mathematical model for the growth and spreading of a metastatic population was developed [43,44] that integrates angiogenesis-mediated primary tumor growth with that at secondary tumor sites.

We present here a new model based on this previous work that integrates systemic inhibition of angiogenesis by a circulating factor, produced by each lesion in a population of tumors. From this model, clinically and biologically relevant quantities can be derived and studied such as the number of the

metastases, the global metastatic burden and the mean size of the secondary colonies.

The model takes into account the local and systemic actions of angiogenesis regulators just described, and is fitted to preclinical data of tumor growth and metastatic development of a breast cancer cell line. Information on the behavior of metastases is inferred from the estimated parameters. Simulations of the cancer history are performed which provide a detailed description of the distribution of the tumors in size and compare metastatic development theories, including those that incorporate systemic inhibition of angiogenesis (SIA). The model is then used to test the biological hypothesis of a global dormancy state of self-inhibiting tumors and identify corresponding ranges of the inhibitor production rate. This hypothesis could yield further understanding of the reported clinical data from [1,3,5], which suggest that a large proportion of the population has occult dormant tumors that remain small and asymptomatic over an extended period, possibly longer than the life span. This fact could be due to a global, self-systemic inhibition of tumor angiogenesis, resulting in a stable homeostatic total metastatic burden.

Model

The global philosophy of the model we propose is to consider the development of cancer disease at the organism scale, by describing the growth and spreading of the population of secondary tumors (metastases) as well as the primary, taking into account organism-scale signaling interactions amongst these various tumor sites. The impetus for this viewpoint comes from [42] where the authors derived a structured population model for describing the metastatic colonies represented by a density structured in size (volume). This model consists of a linear transport partial differential equation with a nonlocal boundary condition of renewal type. It has been further mathematically studied in [45,46], in particular to develop efficient numerical methods for discretizing the problem.

A major limitation of this model is that it does not take angiogenesis into account, although this is a fundamental process of tumor development that cannot be ignored, particularly if we want to study the effects of angiogenic inhibition. By combining the approach of [42] with the model of [10] for tumor growth under angiogenic control, we developed in previous work a new model taking into account the angiogenic process in the growth of each tumor [43,44,47]. This model integrates all the basic fundamental features of a cancer disease: proliferation, angiogenesis and metastatic spreading. Combined to the fact that it is written at the level of the organism makes it an adapted framework for modeling systemic inhibition of angiogenesis (SIA) viewed as inhibiting interactions across a population of tumors.

A schematic view of the new model we propose for SIA is presented in the Figure 1. The main feature added to the previous model from [47] is a new variable representing the circulating concentration of an endogenous angiogenesis inhibitor standing for all possible inhibitory molecules (examples being

endostatin, angiostatin and thrombospondin-1). It impacts on the growth of each tumor. As a general modeling principle, we want to be parsimonious and describe the major dynamics of the system with as few parameters as possible.

To begin the model description, tumors are seen as individuals whose state is described by two traits: volume V and carrying capacity K. The primary tumor state is denoted $(V_p(t), K_p(t))$. The model's main variable is $\rho(t, V, K)$, the physiologically structured density of metastases with volume V and carrying capacity K at time t. The term density means that the metastases are assumed to live in a continuum of sizes and carrying capacities and that the number of tumors between volumes V_1 and V_2 and carrying capacities between K_1 and K_2 is given by $\int_{V_1}^{V_2}\int_{K_1}^{K_2}\rho(t,V,K)dVdK$. We assume that the dynamics of each tumor's state are governed by a growth rate $G(V,K;V_p,\rho)$, that spreading of new metastases is driven by an emission rate $\beta(V)$ and that the repartition of metastases at birth is given by $N(\sigma)$. The precise expressions of these functions will be described below. We consider some fixed final time T and a physiological domain $\Omega =]V_0, +\infty[\times]0, +\infty[$ where the distribution of metastases has its support, which means that metastases have size bigger than the size of one cell V_0 and non-negative carrying capacity. The function $\nu(\sigma)$ stands for the external normal to the boundary $\partial\Omega$ of the domain, for $\sigma = (V, K), \sigma \in \partial\Omega$. We use the notation $\partial\Omega^+$, for the subset of the boundary where the flux is entering, i.e. where $G(t,\sigma)\cdot\nu(\sigma) < 0$. The function ρ^0 is the initial distribution of the metastatic colonies.

Overall, the model is a nonlinear transport partial differential equation of renewal type with a nonlocal boundary condition.

$$(1)\qquad \begin{cases} \partial_t\rho + \mathrm{div}(\rho G) = 0 &]0,T[\times\Omega \\ -G(t,\sigma)\cdot\nu(\sigma)\rho(t,\sigma) = N(\sigma)\left\{\int_\Omega \beta(V)\rho(t,V,K)dVdK + \beta(V_p(t))\right\} &]0,T[\times\partial\Omega^+ \\ \rho(0,V,K) = \rho^0(V,K) & \Omega \end{cases}$$

Tumor growth model

We assume that the primary tumor and the metastases have the same structural growth model but different parameters, due to the different sites where they are located. However, all the metastases are assumed to have the same growth parameters. The growth velocity of each tumor is given by $G(V, K; V_p, \rho)$. Following the approach of [10] we take

$$G(V,K;V_p,\rho) = \begin{pmatrix} aV\ln\left(\dfrac{K}{V}\right) \\ Stim(V,K) - Inhib(V,K;V_p,\rho) \end{pmatrix}$$

where a is a constant parameter driving the proliferation kinetics of the cancer tissue. In the previous expression, the first line is the rate of change of the tumor volume V and the second line is the rate of change of the carrying capacity K. The main idea of this tumor growth model is to start from a gompertzian growth of the tumor volume (or any carrying capacity-like growth model [48]) and to assume that the carrying capacity K is a dynamical variable representing the tumor environment limitations (here limited to the vascular support) that changes in time. The balance between a stimulation term $Stim(V,K)$ and an inhibition term $Inhib(V,K;V_p,\rho)$ governs the dynamics of the carrying capacity. For the stimulation term we follow [10] and take

$$Stim(V,K) = bV$$

where the parameter b is related to the concentration of angiogenic stimulating factors such as VEGF or bFGF. This last quantity was derived to be constant in [10] from the consideration of very fast clearance of angiogenic stimulators [34].

For the inhibition term, Hahnfeldt et al. [10] only considered a local inhibition coming from the tumor itself. Our main modeling novelty is to consider in addition a global inhibition coming from the release in the circulation of angiogenic inhibitors by the total (primary + secondary) population of tumors. The following is an extension of the biophysical analysis performed in [10]. Let us consider a spherical tumor of radius R inside the host body. The host is represented, for simplicity, by a single compartment of volume V_d in which concentrations are assumed spatially uniform. Let $n(r)$ be the inhibitor concentration inside the tumor at radial distance r. Let the intra-tumor clearance be zero [10]. At quasi steady state, $n(r)$ solves the following diffusion equation:

$$n''(r) + \frac{2n'(r)}{r} + \frac{p}{D^2} = 0$$

where p is the inhibitor production rate and D^2 is the inhibitor diffusion constant. This equation is endowed with the boundary condition $n(R) = i(t;V_p,\rho)$, $i(t;V_p,\rho)$ being the systemic concentration of the inhibitor. Solving this equation (using that $n(0) < +\infty$) we obtain

$$n(r) = i + \frac{p}{6D^2}(R^2 - r^2)$$

From this expression we compute the mean inhibitor concentration in the tumor to obtain

$$Inhib(V,K;V_p,\rho) = \hat{e}\left(i + \frac{p}{15D^2}R^2\right)K = \hat{e}\left(i + \frac{p}{15D^2}\left(\frac{3}{4\pi}\right)^{2/3}V^{2/3}\right)K$$

where $\hat{e}$ is a sensitivity coefficient. For i, considering that the total flux of inhibitors produced by a tumor with volume V is pV and assuming that the inhibitor production rate is the same in all the tumors, we have

$$V_d \frac{di}{dt} = pV_p + \int_\Omega pV\rho(t,V,K)dVdK - kV_d i$$

with k an elimination constant from the blood circulation. Setting $I(t;V_p,\rho) = V_d i(t;V_p,\rho)$, we get

$$\frac{dI}{dt} = pV_p + \int_\Omega pV\rho(t,V,K)dVdK - kI$$

Overall, the explicit expression of the metastases growth rate is

$$G(V,K;V_p,\rho) = \begin{pmatrix} aV\ln\left(\frac{K}{V}\right) \\ bV - dV^{2/3}K - eIK \end{pmatrix} \tag{2}$$

where $e = \frac{\hat{e}}{V_d}$ and

$$d \coloneqq eV_d \frac{p}{15D^2}\left(\frac{3}{4\pi}\right)^{2/3} \tag{3}$$

Notice that we retrieve here the local term $dV^{2/3}$ from the analysis of (10) and that a global term eI is added for the effect of systemic inhibition of angiogenesis.

For the primary tumor, we assume the same structural growth model: the dynamics of $(V_p(t), K_p(t))$ are given by

$$\frac{d}{dt}\begin{pmatrix} V_p \\ K_p \end{pmatrix} = G_p(V_p,K_p;V_p,\rho) \tag{4}$$

endowed with some suitable initial conditions. However, in the last equation we assume values of growth parameters different from those characterizing metastases, that is parameters a_p and b_p are possibly different from a and b. The inhibitor production rate p and effect of the inhibitor e are assumed to be the same for the primary and secondary tumors, which implies same value also for d in view of formula (3).

Metastatic spreading

There is no clear consensus in the literature about metastases being able to metastasize or not [49–51]. However, cancer cells that acquired the ability to metastasize should conserve it when establishing in a new site. Moreover, since metastasis is a long process before being detectable [49–51] (in particular because tumors could remain dormant during large time periods), the absence of

clear proof in favor of metastases from metastases could be due to the short duration of the experiments compared to the time required for a secondary generation of tumors to reach a visible size. Here we are interested in long time behaviors and, although metastases from metastases could be neglected in first approximation, we think this second order term is relevant in our setting and chose to include it in our modeling, following clinical evidences of second-generation metastases [52].

Successful metastatic seeding results from one malignant cell being able to overcome various adverse events: detachment from the tumor, intravasation, survival in the blood/lymphatic circulation, escape from immune surveillance, extravasation, survival in a new environment, (see [53] for more details). We regroup all these events into one emission rate $\beta(V,K)$ quantifying the number of successfully newly created metastases per unit of time, and neglect intricate description of all these processes. We assume that very small metastases do not metastasize because they don't have access to the blood circulation and hence include a threshold V_m below which tumors don't spread new individuals (taken to be 1 mm^3 as an approximation of the volume at which the angiogenic switch happens). Apart from the addition of this threshold, the expression of β is taken from [42]:

$$\beta(V,K) = \beta(V) = mV^{\alpha}1_{V\geq V_m} \tag{5}$$

where m and α are coefficients quantifying the intrinsic metastatic potential of the cancer disease. The parameter α is between 0 and 1 and is the third of the fractal dimension of the vasculature of the tumor under consideration, here assumed to be an intrinsic feature of the development of all the tumors in the cancer disease. For instance, if vasculature develops superficially then $\alpha = 2/3$, whereas a fully penetrating vasculature would give a value of $\alpha = 1$. We chose to model only dependence on the volume and not on the carrying capacity since previous simulations showed that adding a monotonous dependence on K did not improve the flexibility of the model in simulations but added at least one parameter, in opposition to our parsimony principle.

Stating a balance law for the number of metastases when growing in size gives the first equation of (1). The boundary condition, i.e. the second equation of (1), states that the entering flux equals the newly born metastases. These result from two sources: spreading from the primary tumor is represented by the term $\beta(V_p(t))$ and second generation tumors coming from the metastases themselves are described by the term $\int_{\Omega} \beta(V)\rho(t,V,K)dVdK$. The map $\sigma \mapsto N(\sigma), \sigma = (V,K) \in \partial\Omega$ stands for the volume and carrying capacity distribution of metastases at birth. We assume that newly created tumors have all the size of 1 cell denoted by V_0 and some initial carrying capacity denoted by K_0 and thus take

$$N(\sigma) = \delta_{\sigma=(V_0,K_0)} \tag{6}$$

i.e. the Dirac distribution centered in (V_0, K_0). We allow metastases to exit the domain by imposing the boundary condition only where the flux points inward.

In view of expression (2), the growth velocity could push out tumors with carrying capacity less than one cell. This occurs when global inhibition is strong enough, i.e. when $bV_0 - dV_0^{\frac{5}{3}} - eIV_0 < 0$. These tumors are removed from the population under consideration and this corresponds to the death of one-cell metastases caused by nutrient deprivation. We refer to [44,54] for more detailed modeling considerations about the boundary condition.

From the solution ρ of the mathematical model (1,3-6), we can define relevant biological quantities such as the total number of metastases: $N(t) = \int \rho(t,V,K)dVdK$, the number of metastases with size above some given threshold V_τ (to compute the number of detectable metastases or only the large ones for instance): $\int_{V \geq V_\tau} \rho(t,V,K)dVdK$, the total metastatic burden: $M(t) = \int_\Omega V\rho(t,V,K)dVdK$ or the mean size of the metastases: $\frac{M(t)}{N(t)}$.

Numerical method

To approximate the solutions of the problem (1,3-6) we adapted a numerical method previously developed for the model without SIA in [44,54]. It is a lagrangian scheme based on the straightening of the characteristics of the transport equation. We used an Euler method for discretization of the characteristics and computation of the primary tumor ODE. The integral in the boundary condition was computed using the trapezoid rule.

Results

Parameter values and confrontation to preclinical data

Data about metastatic development are not common in the literature, especially for micro-metastases or dormant tumors since these measurements are technically hard to obtain. Even more difficult to find are data quantifying systemic inhibition of angiogenesis. For our purpose we use data from Huang et al. (54) that do not explicitly deal with systemic inhibition of angiogenesis nor global dormancy but where number and mean size of metastases at the end time (T=32 days) are available, together with the primary tumor growth in time. The cell line used in this work is the 4T1 (spontaneous mouse breast cancer), known to be highly metastatic with relatively slow primary tumor growth, injected subcutaneously (10^5 cells) in BALB/c mice. As shown in the following, the model was able to appropriately describe these data.

Values of the parameters were fixed either by direct extraction from the literature, heuristic derivation or by fitting the model to the data from [55]. Notice that for the preclinical data that we use, metastases actually develop to symptomatic volumes and we are not in presence of a manifest global inhibition. Hence for fitting of the model, we consider SIA as being negligible and take $I = 0$. The parameter estimation we performed is only intended for estimation of growth and metastatic spreading parameters. Assumption of negligible SIA was

found *a posteriori* to be relevant for description of the data from [55], because adding an SIA term did not have any impact on the model simulations, in the framework of the experiment from [55]. In the context of no SIA, there is no impact of the metastases on the primary tumor and we fitted separately the primary tumor growth and the metastatic development. This approach (compared to a global fitting of all the parameters together) reduces the over-parameterization of the model and allows for more stable and biologically relevant parameters estimation. Indeed, only two degrees of freedom are used to fit the primary tumor growth (seven time points) and two for the data on metastases (two measurements). The values, units and meaning of the model parameters are summarized in the Table 1.

Heuristic derivations from the literature

In [10] we can find values for the elimination rates k and efficacy constants e for two endogenous angiogenesis inhibitors, namely endostatin and angiostatin. These values were obtained by fitting tumor growth data of mice that received injections of these anti-angiogenic agents. We focus here on angiostatin and convert in day^{-1}/mg the value of e from [10] given in day^{-1}/(mg/kg) by assuming a mouse weight of 20 g. We take the same elimination rate k from the blood circulation as in this paper. It is worth noticing that this value gives a half life for angiostatin of 1.8 days, which is consistent with the value of 2.5 days that can be found in [26].

In [26], it is shown that injection of 12.5 µg per day of recombinant human angiostatin reproduces the systemic inhibition due to a primary tumor removed when it reached the size of 1500 mm^3. Hence an approximation of the production rate in their setting is $p \simeq \frac{12.5}{1500} \times 10^{-3} \simeq 8.3 \times 10^{-6}$ mg.mm^{-3} day^{-1}. The blood volume in mouse is about 1.2-1.6 cm^3 per 20 g body weight, let us say 1.4 cm^3. Assuming that the interstitial space be 30% of the extravascular space (in agreement with measurements of the fraction of volume occupied by cells), by summing interstitial (extracellular) space to blood volume we obtained 6.98 cm^3. So we took $V_d = 7000$ mm^3 as an approximation of the distribution volume. For the diffusion coefficient of angiostatin D^2 we used the value in [56] after conversion in mm^{2}day^{-1}, which gives 1.56 mm^{2}day^{-1}. Based on these values and the formula (3) for d derived in the modeling section, we were able to heuristically derive an approximation of $d \simeq 0.0717$ mm^{-2} day^{-1}. Hence we fixed d and d_p to this value, which allowed us to reduce possible indetermination in the estimation of b and d in the growth model.

When reproducing Huang et al's experiment, we fixed the initial size of the primary tumor to $V_{0,p}$ = 10^5 cells = 0.1 mm^3 (number of injected cells to the mouse) and arbitrarily set the initial carrying capacity of the primary tumor to $K_{0,p}$ = 200 mm^3. Metastases were assumed to start with initial size V_0 = 1 cell = 10^{-6} mm^3 and initial carrying capacity K_0 = 1 mm^3 (maximum reachable size without angiogenesis [32]). For metastatic emission, we considered a superficial vascular development and took $\alpha = 2/3$, similarly to the value obtained in (41) from clinical data.

Fit to the data

Parameters a_p and b_p were obtained by minimizing the sum of square errors between the tumor growth model simulation and the primary tumor growth data from [55]. Sum of least squares minimization was performed using the trust region reflective algorithm implemented in Matlab (Matlab 2009b, The Mathworks Inc.). We obtained good adequacy between the fit and the data (Figure 2). Goodness of the fit can be quantified by the R^2 value, $R^2 = 1 - \frac{\sum(y_i - f(t_i))^2}{\sum(y_i - \bar{y})^2}$, where the y_i are the data points, $\bar{y}$ is the mean value of the data and the $f(t_i)$'s are the values of the model at times t_i. The fit we obtained gave $R^2 = 0.99$.

Assuming that differences in the growth between primary tumor and metastases should arise from interactions with the microenvironment, we fixed the proliferation parameter a for the metastases to the value obtained for the primary tumor growth. Parameters b and m were determined by fitting the model to the metastatic data of Huang et al. [55], whose results are reported in Table 2. In [55], data on the size of metastases was given in terms of diameters of the lesion. We converted this value in volume by assuming a width $w = \frac{3}{4}D$, where D is the tumor diameter and using the common formula $V = \frac{\pi}{6} \times D \times w^2$ that supposes the tumor has the shape of an ellipsoid. We obtained good agreement to the number and mean size of metastases, but could not very well describe the proportion of large metastases (>3 mm in diameter). However, the value of the model is still of the order of the data. With this value of m a tumor of 200 mm^3 spreads a new metastasis every 0.77 days.

Simulation of the experimental setting of [55] using the parameters resulting from the model's fit (and $I = 0$) gives further insights on the time development of the metastases and their size distribution at the end. Figure 3.A shows the metastatic burden versus time and Figure 3.B the colonies size distribution at T=32 days for an *in silico* replicate of the experiment performed in[55]. It reveals a nontrivial size distribution of the metastatic colonies at the end with a mode between 0.01 and 0.1 mm^3, and only one tumor with size larger than 10 mm^3. At this time the total lung metastatic burden is 63.5 mm^3 distributed between 48.5 tumors. Simulation performed with non-zero I and the value of p extracted from [26] (see above) presented no significant difference in this setting compared to the simulation with $I = 0$, hence justifying *a posteriori* our assumption of negligible effect of SIA in the setting of [55], used to perform robust estimation of the parameters.

From these simulations and parameter estimation, our mathematical model is a possible theory describing growth and development of primary and secondary tumors in a 4T1 cell line model. Systemic inhibition of angiogenesis had no significant importance in this context with small time range. The structural model endowed with adequate parameter values yields an interesting

theoretical tool to investigate a range of different situations for SIA than the mere experimental setting of [55].

Simulation of the cancer history predicts large metastatic burden

Based on the parameters estimated in the previous section (Table 1), we simulated a cancer history, starting from one initial cancerous cell (and initial carrying capacity of 1 mm^3) until the metastatic burden reaches 5000 mm^3, volume considered to be possibly lethal for the mouse. The simulation predicted this to happen 62.7 days after the first primary tumor cancer cell. Time development of the primary tumor volume, metastatic burden, total number and mean size of metastases as well as inhibitor amount in the host are plotted in Figure 4.

Interestingly, the model simulation predicts that the metastatic burden would overcome the primary tumor (PT) mass, implying that the mouse would probably die from growth of its secondary lesions rather than from the initial tumor. This is consistent with the very metastatically aggressive phenotype of the 4T1 cell line. Quantification of the number of metastases reveals a final number of about 217, lots of them being small (Figure 4C) and probably undetectable in an experimental setting.

Simulation with the same set of parameters but neglecting the effect of SIA ($I = 0$) showed no detectable difference on this time frame. Significant changes are observed later on, for volumes that are not considered to be physiologically relevant. This confirms that for the 4T1 cell line, metastases do develop and do not exhibit global dormancy, even when SIA is present with the inhibitor production parameter value extracted from [26].

Based on biologically relevant parameters, our simulation results suggest large growth of the metastatic burden for the 4T1 cell line when starting from the first cancer cell, with a final metastatic volume larger than the primary tumor.

Higher production of systemic angiogenesis inhibitor could result in long-term stable global dormancy in a population of self-inhibiting metastases

The previous simulations use parameter values derived from experimental data of a situation were metastases do develop and grow, because this is the only case where metastases are measurable and data are available. However we are interested in global dormancy and situations where the metastatic population would remain ultimately small. We postulate that this could happen when production of the angiogenesis inhibitor, represented by parameter p in our model, is significantly higher. Simulation results plotted in Figure 5 were obtained with a value of $p = 2.5\times10^{-4}\text{mg} \cdot \text{mm}^{-3} \cdot \text{day}^{-1}$, i.e. about 30 times the value that we extracted from [26]. From our previous modeling analysis and formula (3), higher production of inhibitor also proportionally increases the local inhibition parameters d and d_p. We kept all the other parameter values

unchanged (Table 1), initial PT volume $V_{0,p}$= 1 cell and initial PT carrying capacity $K_{0,p} = 1$ mm^3. We simulated during a large time of 350 days, hence possibly covering the lifespan of a mouse after appearance of an initial malignant cell. We focused on asymptotic behavior and possible convergence of the system to a steady state. In the Figure 5 are plotted the primary tumor volume, number and total burden of the metastases, the time evolution of the global inhibitor quantity and the size distribution of the metastases at the end time.

In this context, the first cancer cell initiates the disease by growing and generating a first pool of metastases, but these then take the control over the growth of the primary lesion (Figure 5.A). The primary tumor reaches a maximal size of 21.2 mm^3 at time 82.9 days (Figure 5.A) but then shrinks due to inhibition of angiogenesis provoked by the distant metastases. The population of metastases is then left alone and we can appreciate the dynamics of these interacting tumors. There is a slowdown and eventually stabilization of the metastatic burden, with end value of about 2200 mm^3. The burden is composed of a large number of metastases (Figure 5.B), most of them being occult micro-metastases as can be seen on the end size distribution (Figure 5.C). This interesting feature of the model simulation could be an *in silico* replicate of the aforementioned situations of cancer without disease [5]. In our model it translates into an asymptotical steady state for the metastatic burden composed of small lesions. The general dynamics of the metastatic burden results from the balance of two stimulating forces (growth and spread of new individuals) and an inhibiting one (systemic inhibition of angiogenesis). Stimulation depends on parameters a and b for the growth process and m and α for the spreading, while the inhibition depends on p (that indirectly controls the value of d), e and k. The present values of the parameters generated long-term stabilization of the mass. The size distribution of the population of secondary tumors at time T = 350 days reveals to be non trivial, with different numbers in the various size ranges. All of the metastases have volume lower than 10 mm^3.

Assuming a large production of systemic inhibition of angiogenesis we theoretically obtained *in silico* an important population of dormant micro-metastases inhibiting each other's growth, with a possibly non-lethal final total metastatic burden. This situation can be reached with an at least 30 fold higher value of the inhibitor production parameter p, as compared to the value estimated from [26].

Discussion

We have introduced an organism-scale model for development of a primary tumor and a population of secondary tumors that takes into account systemic inhibiting interactions between the tumors due to the release of a circulating angiogenic inhibitor.

The model proved to be able to describe *in vivo* data of primary tumor and metastatic development and allowed to infer information such as the size density

distribution of metastases that are not completely accessible in experimental settings.

Our mathematical model endowed with biologically relevant parameter values able to reproduce experimental measurements, yields an interesting tool for theoretical study of metastatic dynamics. It was used to investigate the whole cancer history from the first cancer cell and predicted that for the metastatically aggressive 4T1 cell line, metastases would grow unbounded for physiologically relevant set of values. The total metastatic burden would become larger than the primary tumor mass and probably be responsible for death of the animal. SIA effects were found to be negligible in this context.

Higher production rate of the inhibitor could make the primary tumor appearance and growth only a transient event starting a larger process of metastatic development where, due to self-inhibition of angiogenesis at the organism scale, global dormancy is imposed to the entire population and the metastatic burden asymptotically stabilizes to an asymptomatic state of the cancer disease. This shows that SIA is qualitatively able to generate a situation of global dormancy. However this situation could be obtained with a very high value of inhibitor production rate (30 fold the value extracted from [26]) that seems not to be physiological. This suggests that SIA alone is probably not sufficient to induce global dormancy and other processes (such as immune effects) are probably significantly involved.

The simulations and predictions based on our model warrant further biological investigation of metastatic dormancy. The quantitative distinction between SIA and no SIA theories could give information about relevance of this phenomenon in experiments looking at the time development of a cancer disease in mice. The hypothesis that we propose in this paper (organism-scale metastatic dormancy maintained by self-inhibition of a population of tumors) could be experimentally tested by injecting a systemic inhibitor in a mouse model of metastases, in quantities predicted by the model to induce global dormancy and compare to another group where quantities injected are predicted not to be sufficient to induce global dormancy. Experimental results could then be compared to the model's predictions.

Translating our results to human situations, they could give elements of explanation to the occult tumors found in autopsy studies and would reinforce the fact that a large part of the population bears numerous metastases that remain asymptomatic because they are dormant. Their dormancy could be due to systemic angiogenesis inhibiting molecules that prevent the development of neo-vasculature and ensure homeostasis of the global cancer tissue.

Development of a cancer disease in individuals having a low production of inhibitor could hence be prevented by external administration of supplementary inhibitory agents that could maintain an existing population of tumors in a global dormancy state. This preventing approach was also reviewed in [57].

The modeling approach we used was based on biophysical heuristic considerations due to the lack of data in the literature on systemic inhibition of angiogenesis among tumors. A more precise model is currently being developed based on experiments of tumor-tumor interactions performed in our lab. Also, for parsimony reasons, we did not include the effects of immune surveillance in the model, although this process might be relevant in the context of global dormancy. We intend to address this in future work.

Mathematically, the model is a nonlinear renewal equation whose general dynamics is much richer than the model without interactions between the individuals. In particular, simulations suggest that this model could exhibit convergence to a nontrivial stable steady state. Mathematical analysis of such a nonlinear transport equation with a non-local term in the velocity is not classical and, as far as we know, well-posedness of the problem and study of the asymptotic behavior cannot be directly derived from the existing literature and are open problems. We also plan to address these issues in future work.

Acknowledgements

The authors would like to thank Dr A. d'Onofrio for useful discussions.

References

1. Welch HG, Black WC (2010) Overdiagnosis in cancer. J Natl Cancer Inst 102: 605–613.

2. Black WC, Welch HG (1993) Advances in diagnostic imaging and overestimations of disease prevalence and the benefits of therapy. N Engl J Med 328: 1237–1243.

3. Nielsen M, Thomsen JL, Primdahl S, Dyreborg U, Andersen JA (1987) Breast cancer and atypia among young and middle-aged women: a study of 110 medicolegal autopsies. Br J Cancer 56: 814–819.

4. Sánchez-Chapado M, Olmedilla G, Cabeza M, Donat E, Ruiz A (2003) Prevalence of prostate cancer and prostatic intraepithelial neoplasia in Caucasian Mediterranean males: an autopsy study. Prostate 54: 238–247.

5. Folkman J, Kalluri R (2004) Cancer without disease. Nature 427: 787.

6. Aguirre-Ghiso JA (2007) Models, mechanisms and clinical evidence for cancer dormancy. Nature Reviews Cancer 7: 834–846.

7. Almog N (2010) Molecular mechanisms underlying tumor dormancy. Cancer Lett 294: 139–146.

8. Holmgren L, O'Reilly M, Folkman J (1995) Dormancy of micrometastases: balanced proliferation and apoptosis in the presence of angiogenesis suppression. Nat Med 1: 149–153.

9. Almog N, Henke V, Flores L, Hlatky L, Kung AL, et al. (2006) Prolonged dormancy of human liposarcoma is associated with impaired tumor angiogenesis. FASEB J 20: 947–949.

10. Hahnfeldt P, Panigraphy D, Folkman J, Hlatky L (1999) Tumor development under angiogenic signaling: a dynamical theory of tumor growth, treatment, response and postvascular dormancy. Cancer Res 59: 4770–4775.

11. Retsky MW, Demicheli R, Hrushesky WJM, Baum M, Gukas ID (2008) Dormancy and surgery-driven escape from dormancy help explain some clinical features of breast cancer. APMIS 116: 730–741.

12. Retsky M, Demicheli R, Hrushesky W, Baum M, Gukas I (2010) Surgery triggers outgrowth of latent distant disease in breast cancer: an inconvenient truth? Cancers 2: 305–337.

13. Brackstone M, Townson JL, Chambers AF (2007) Tumour dormancy in breast cancer: an update. Breast Cancer Res 9: 208.

14. Ossowski L, Aguirre-Ghiso JA, Manuscript A (2010) Dormancy of metastatic melanoma. Pigment Cell Melanoma Res 23: 41–56.

15. Prehn RT (1993) Two competing influences that may explain concomitant tumor resistance. Cancer Res 53: 3266–3269.

16. Chiarella P, Bruzzo J, Meiss RP, Ruggiero RA (2012) Concomitant tumor resistance. Cancer Lett 324: 133–141.

17. Ehrlich P (1905) Beobachtungen über maligne Mäusetumoren. Berliner Klinische Wochenschrift 42: 871–874.

18. Dewys WD (1972) Studies correlating the growth rate of a tumor and its metastases and providing evidence for tumor-related systemic growth-retarding factors. Cancer Res 32: 374–379.

19. Gunduz N, Fisher B, Saffer E a (1979) Effect of surgical removal on the growth and kinetics of residual tumor. Cancer Res 39: 3861–3865.

20. Fisher B, Gunduz N, Saffer EA (1983) Influence of the interval between primary tumor removal and chemotherapy on kinetics and growth of metastases. Cancer Res 43: 1488–1492.

21. Gorelik E (1983) Resistance of tumor-bearing mice to a second tumor challenge. Cancer Res 43: 138–145.

22. Li TS, Kaneda Y, Ueda K, Hamano K, Zempo N, et al. (2001) The influence of tumour resection on angiostatin levels and tumour growth--an experimental study in tumour-bearing mice. Eur J Cancer 37: 2283–2288.

23. Peeters CFJM, de Waal RMW, Wobbes T, Westphal JR, Ruers TJM (2006) Outgrowth of human liver metastases after resection of the primary colorectal tumor: a shift in the balance between apoptosis and proliferation. Int J Cancer 119: 1249–1253.

24. Peeters CF, de Waal RM, Wobbes T, Ruers TJ (2008) Metastatic dormancy imposed by the primary tumor: does it exist in humans? Ann Surg Oncol 15: 3308–3315.

25. Venderbosch S, de Wilt JH, Teerenstra S, Loosveld OJ, van Bochove A, et al. (2011) Prognostic value of resection of primary tumor in patients with stage IV colorectal cancer: retrospective analysis of two randomized studies and a review of the literature. Ann Surg Oncol 18: 3252–3260.

26. O'Reilly MS, Holmgren L, Shing Y, Chen C, Rosenthal R a, et al. (1994) Angiostatin: a novel angiogenesis inhibitor that mediates the suppression of metastases by a Lewis lung carcinoma. Cell 79: 315–328.

27. O'Reilly M, Boehm T, Shing Y, Fukai N (1997) Endostatin: an endogenous inhibitor of angiogenesis and tumor growth. Cell 88: 277–285.

28. Rofstad E, Graff B (2001) Thrombospondin-1-mediated metastasis suppression by the primary tumor in human melanoma xenografts. J Invest Dermatol 117: 1042–1049.

29. Volpert O V, Lawler J, Bouck NP (1998) A human fibrosarcoma inhibits systemic angiogenesis and the growth of experimental metastases via thrombospondin-1. Proc Natl Acad Sci U S A 95: 6343–6348.

30. Sckell A, Safabakhsh N, Dellian M, Jain RK (1998) Primary tumor size-dependent inhibition of angiogenesis at a secondary site: an intravital microscopic study in mice. Cancer Res 58: 5866–5869.

31. Hanahan D, Folkman J (1996) Patterns and emerging mechanisms of the angiogenic switch during tumorigenesis. Cell 86: 353–364.

32. Folkman J (1971) Tumor angiogenesis: therapeutic implications. N Engl J Med 285: 1182–1186.

33. Folkman J (1995) Angiogenesis inhibitors generated by tumors. Mol Med 1: 120–122.

34. Folkman J (1995) Angiogenesis in cancer, vascular, rheumatoid and other disease. Nat Med 1: 27–31.

35. Araujo RP, McElwain DLS (2004) A history of the study of solid tumour growth: the contribution of mathematical modelling. Bull Math Biol 66: 1039–1091.

36. Fidler IJ, Paget S (2003) The pathogenesis of cancer metastasis: the “seed and soil” hypothesis revisited. Nat Rev Cancer 3: 453–458.

37. Liotta LA, Saidel GM, Kleinerman J (1976) Stochastic model of metastases formation. Biometrics 32: 535–550.

38. Retsky MW, Demicheli R, Swartzendruber DE, Bame PD, Wardwell RH, et al. (1997) Computer simulation of a breast cancer metastasis model. Breast Cancer Res Treat 45: 193–202.

39. Willis L, Alarcón T, Elia G, Jones JL, Wright NA, et al. (2010) Breast cancer dormancy can be maintained by small numbers of micrometastases. Cancer Res 70: 4310–4317.

40. Chen J, Sprouffske K, Huang Q, Maley CC (2011) Solving the puzzle of metastasis: the evolution of cell migration in neoplasms. PloS One 6: e17933.

41. Hanin L (2013) Seeing the invisible: how mathematical models uncover tumor dormancy, reconstruct the natural history of cancer, and assess the effects of treatment. Advances Exp Med Biol 734: 261–282.

42. Iwata K, Kawasaki K, N. S, Shigesada N (2000) A dynamical model for the growth and size distribution of multiple metastatic tumors. J Theor Biol 203: 177–186.

43. Benzekry S, André N, Benabdallah A, Ciccolini J, Faivre C, et al. (2012) Modelling the impact of anticancer agents on metastatic spreading. Math Model Nat Phenom 7: 306–336.

44. Benzekry S (2011) Mathematical and numerical analysis of a model for anti-angiogenic therapy in metastatic cancers. ESAIM: Mathematical Modelling and Numerical Analysis 46: 207–237.

45. Barbolosi D, Benabdallah A, Hubert F, Verga F (2009) Mathematical and numerical analysis for a model of growing metastatic tumors. Math Biosci 218: 1–14.

46. Devys A, Goudon T, Lafitte P (2009) A model describing the growth and the size distribution of multiple metastatic tumors. Discrete and Continuous Dynamical Systems - Series B 12: 731–767.

47. Benzekry S (2011) Mathematical analysis of a two-dimensional population model of metastatic growth including angiogenesis. J Evol Equ 11: 187–213.

48. D'Onofrio A, Gandolfi A (2004) Tumour eradication by antiangiogenic therapy: analysis and extensions of the model by Hahnfeldt et al. (1999). Math Biosci 191: 159–184.

49. Tait CR, Dodwell D, Horgan K (2004) Do metastases metastasize? J Pathol 203: 515–518.

50. Bethge A, Schumacher U, Wree A, Wedemann G (2012) Are metastases from metastases clinical relevant? Computer modelling of cancer spread in a case of hepatocellular carcinoma. PloS One 7: e35689.

51. Sugarbaker E V, Cohen a M, Ketcham a S (1971) Do metastases metastasize? Annals of surgery 174: 161–166.

52. August DA, Sugarbaker PH, Schneider PD (1985) Lymphatic dissemination of hepatic metastases. Implications for the follow-up and treatment of patients with colorectal cancer. Cancer 55: 1490–1494.

53. Gupta GP, Massagué J (2006) Cancer metastasis: Building a framework. Cell 127: 679–695.

54. Benzekry S (2012) Passing to the limit 2D–1D in a model for metastatic growth. J Biol Dynam 6: 19–30.

55. Huang X, Wong MK, Yi H, Watkins S, Laird AD, et al. (2002) Combined therapy of local and metastatic 4T1 breast tumor in mice using SU6668, an inhibitor of angiogenic receptor tyrosine kinases, and the immunostimulator B7.2-IgG fusion protein. Cancer Res 62: 5727–5735.

56. Levine HA, Pamuk S, Sleeman BD, Nilsen-Hamilton M (2001) Mathematical modeling of capillary formation and development in tumor angiogenesis: penetration into the stroma. Bull Math Biol 63: 801–863.

57. Albini A, Tosetti F, Li VW, Noonan DM, Li WW (2012) Cancer prevention by targeting angiogenesis. Nat Rev Clin Oncol: 1–12.

Table 1: Values, units and meaning of the model parameters. PT = Primary Tumor. Met = metastases. I = global amount of angiogenic inhibitor in the blood. H = heuristic derivation

Parameter	Value	Unit	Meaning	Origin
$\mathbf{a_P}$	0.154	day^{-1}	PT cells proliferation	Fit PT
$\mathbf{b_P}$	16.7	day^{-1}	PT angiogenic stimulation	Fit PT
$\mathbf{d_P}$	0.0717	$mm^{-2}\ day^{-1}$	PT angiogenic local inhibition	H
a	0.154	day^{-1}	Met cells proliferation	Fit Met
b	12.5	day^{-1}	Met angiogenic stimulation	Fit Met
d	0.0717	$mm^{-2}\ day^{-1}$	Met angiogenic local inhibition	H
m	0.0229	$mm^{-3}\ day^{-1}$	Colonization rate	Fit Met
$\boldsymbol{\alpha}$	2/3		Fractal dimension of vascularization	[42]
p	$8.3x10^{-6}$	$mg\ mm^{-3}\ day^{-1}$	Production of I	[26]
k	0.38	day^{-1}	Elimination rate of I	[10]
e	7.5	$mg^{-1}\ day^{-1}$	Effect of I	[10]
$\mathbf{V_{0,P}}$	0.1	mm^3	PT initial volume	[55]
$\mathbf{K_{0,P}}$	200	mm^3	PT initial carrying capacity	H
$\mathbf{V_0}$	10^{-6}	mm^3	Met initial volume	H
$\mathbf{K_0}$	1	mm^3	Met initial carrying capacity	[32]
$\mathbf{V_m}$	1	mm^3	Threshold for metastatic emission	H
$\mathbf{D^2}$	0.156	$mm^2 day^{-1}$	Angiostatin diffusion coefficient	[56]
$\mathbf{V_d}$	7000	mm^3	Distribution volume	H

Table 2: Metastatic outputs. Comparison of the fit of the model and the data from [55]**. For the number of metastases, the reported model value is the number of tumors above a minimal visible size that we took to be 10 cells (tumors were counted using a dissecting microscope in** [55]**). Mean size was given as diameter in** [55] **and was converted here into volume using** $V = \frac{\pi}{6} \times D \times w^2$, $w = \frac{3}{4} D$

	Value from [55]	**Computed by the model**
Median number of metastases (range)	43 (4-107)	43.03
Mean size of metastases in mm^3 (range)	1.47 (1.30-1.66)	1.476

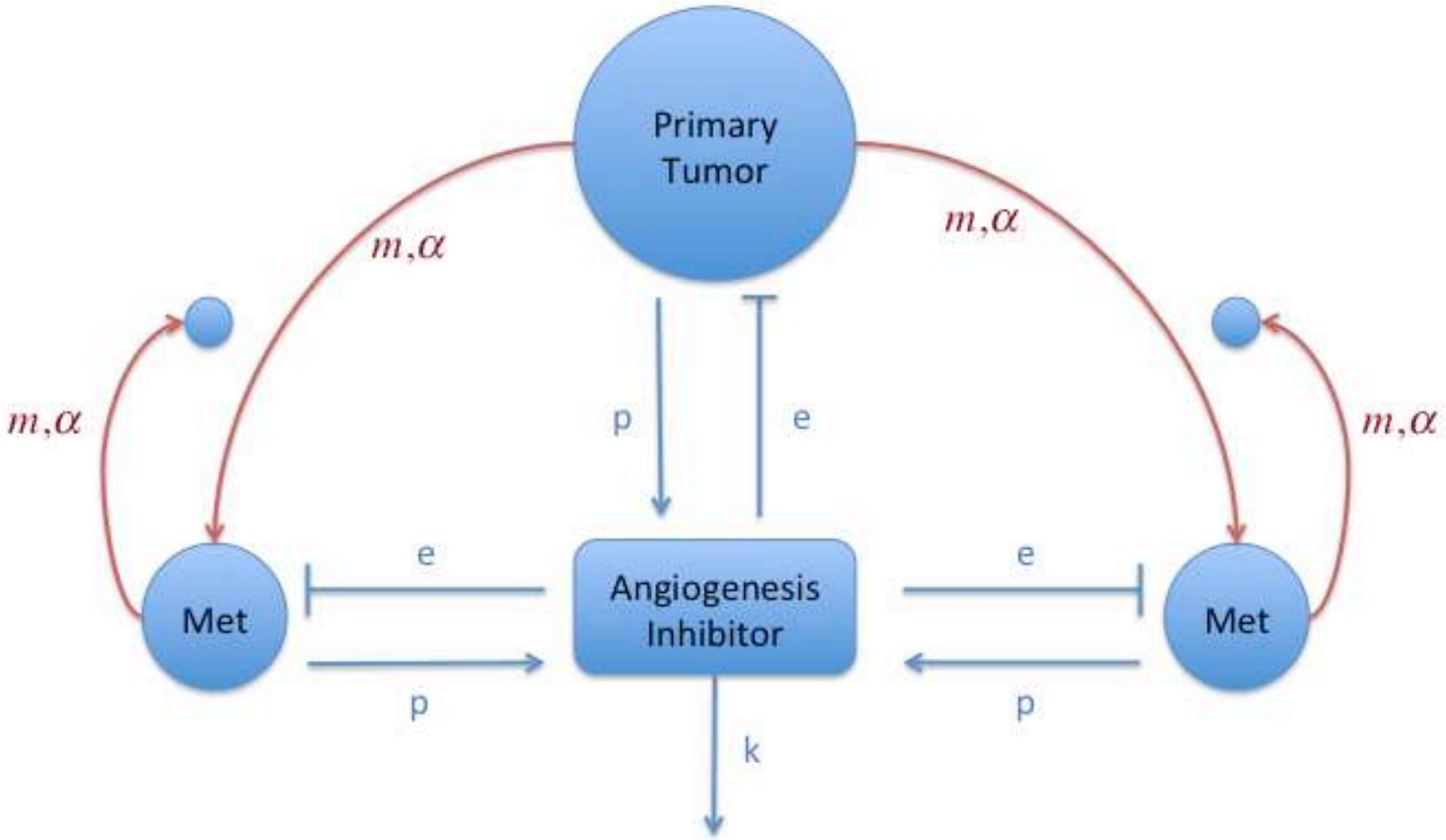

Figure 1: Schematic representation of the model for systemic inhibition of angiogenesis.***m,α***: metastatic spreading parameters. ***p***: production rate of angiogenesis inhibitor.***e***: efficacy parameter of inhibitor. ***k***: elimination rate of the inhibitor.

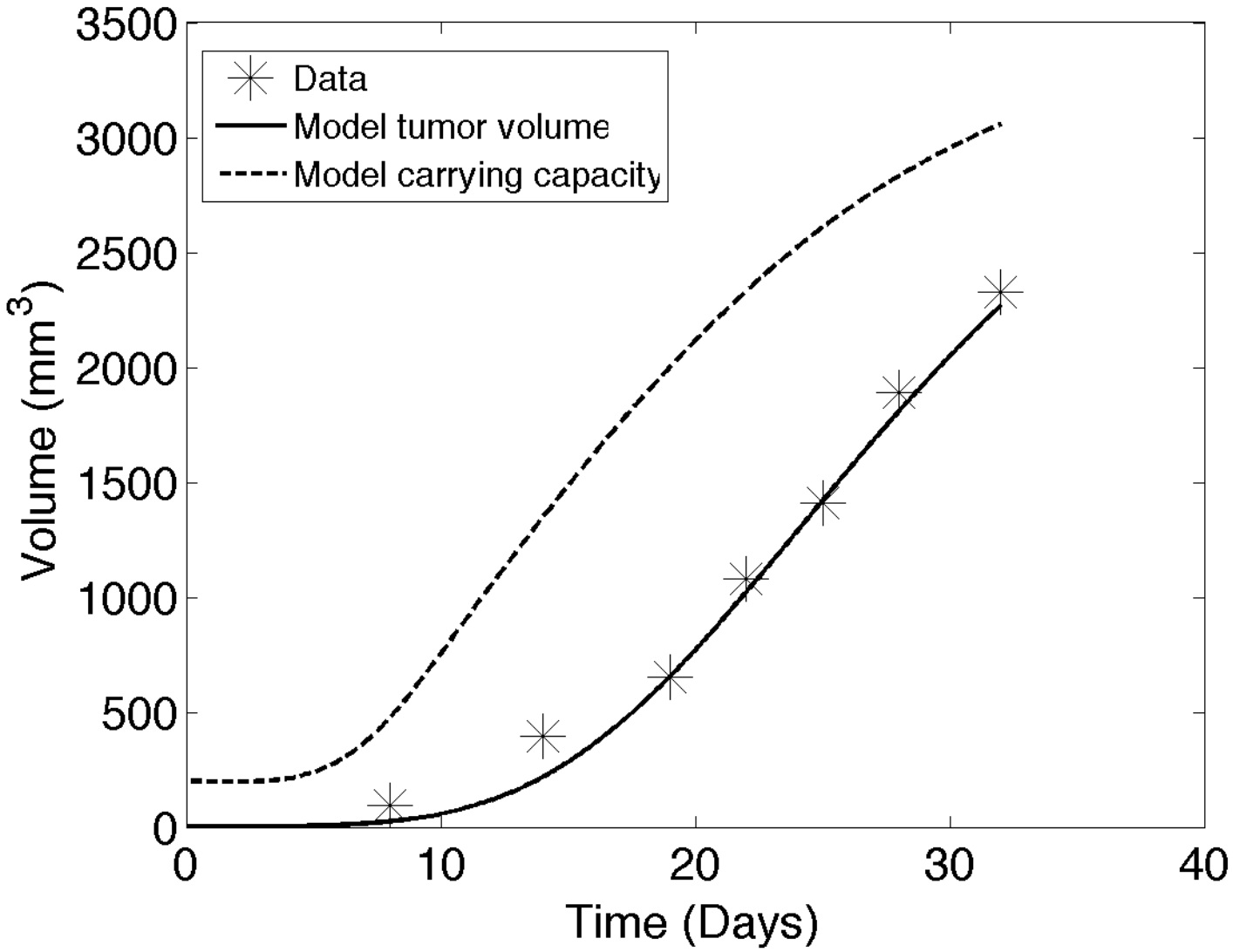

Figure 2: Primary tumor growth. Comparison of the fit of the model and the data from [55]

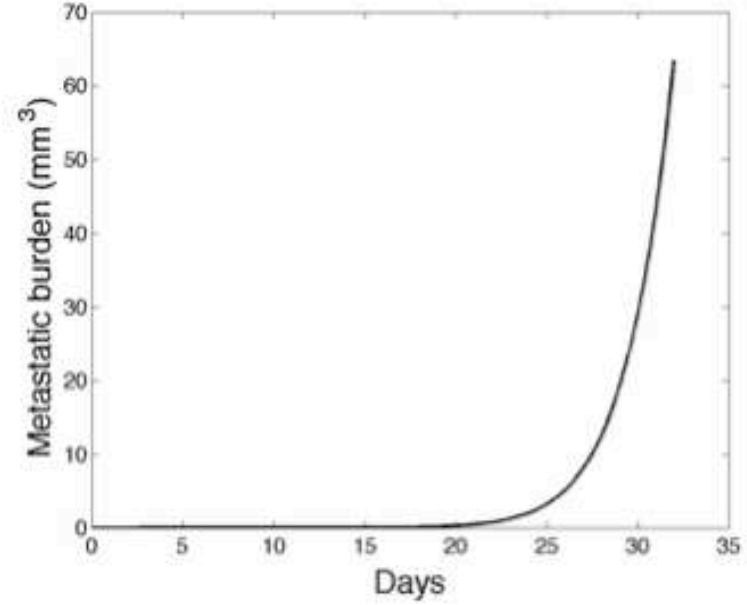

A. Metastatic burden

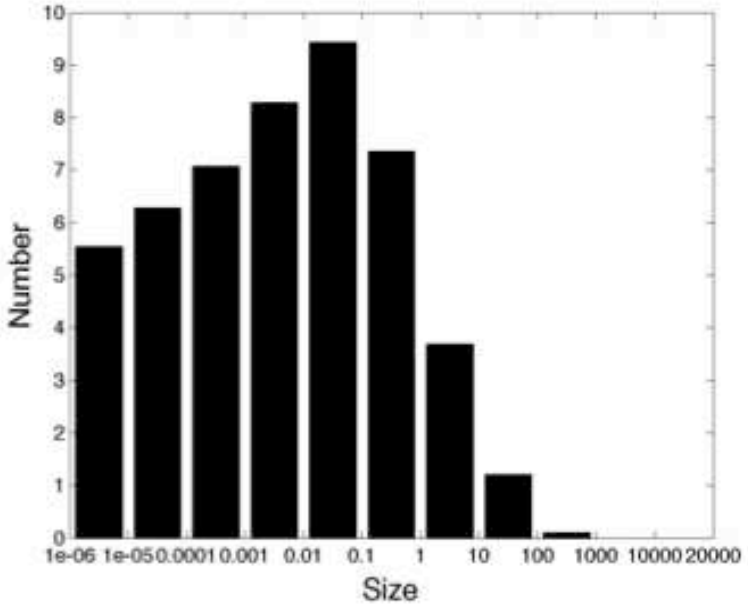

B. Colonies size distribution

Figure 3: *In silico* reproduction of the experiment from [55]. A. Time development of the metastatic burden. B. Colonies size distribution at the end time T=32 days (log-scale on the x-axis).

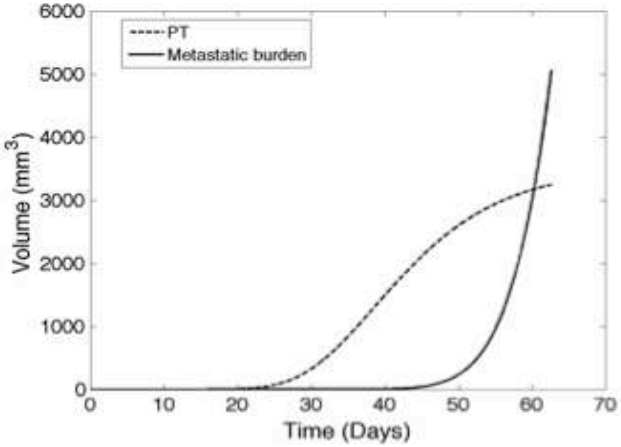

A. PT volume and metastatic burden

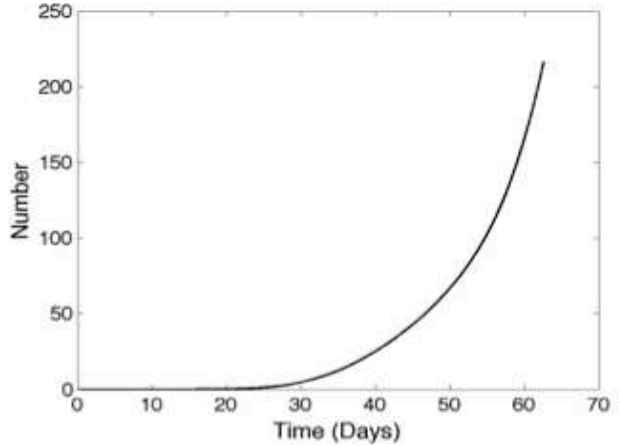

B. Total number of metastases

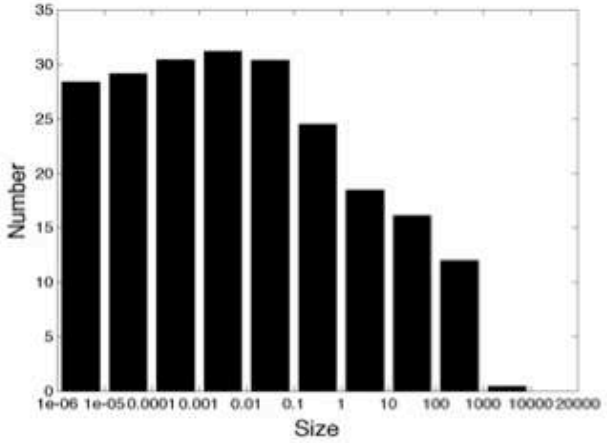

C. End size distribution of metastases

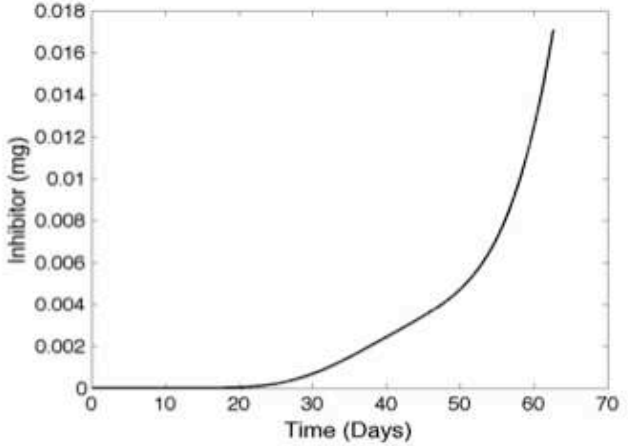

D. Circulating inhibitor

Figure 4: Simulation of the cancer history from the first cancer cell. Parameter values are the ones resulting from the fit to the data of [55], reported in Table 1.

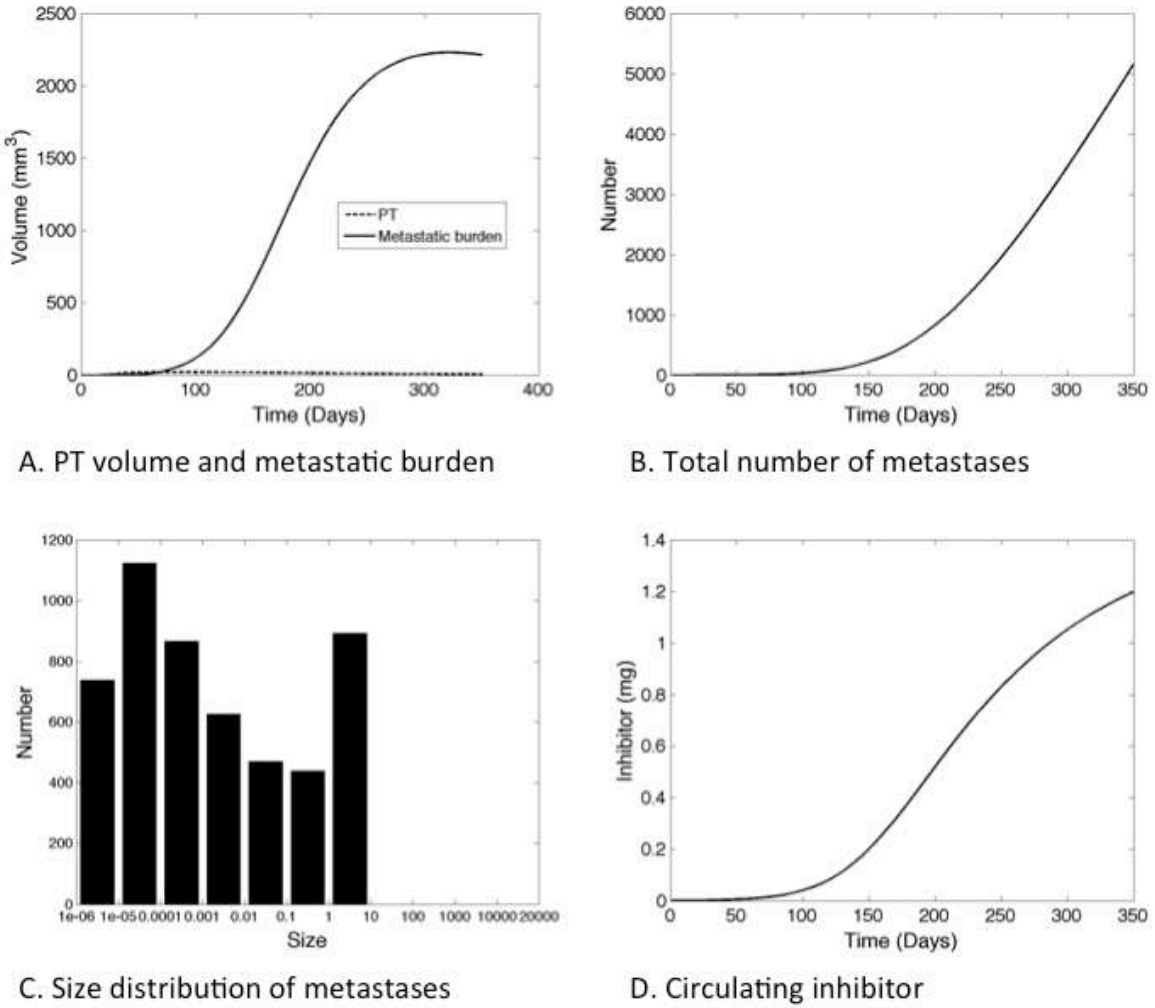

Figure 5: Large time simulation for large inhibitor production ($p = 2.5 \times 10^{-4}$ $mg.mm^{-3}.day^{-1}$, $d=2.16$ mm^{-2} day^{-1}). The model predicts stabilization of the metastatic burden to a situation where the whole metastatic population is in a global dormancy state.